

Repository Istituzionale dei Prodotti della Ricerca del Politecnico di Bari

Surface and bulk hydrophobic cement composites by tyre rubber addition

This is a post print of the following article

Original Citation:
Surface and bulk hydrophobic cement composites by tyre rubber addition / Di Mundo, R., Petrella, A., Notarnicola, M.. - In: CONSTRUCTION AND BUILDING MATERIALS. - ISSN 0950-0618. - ELETTRONICO. - 172:(2018), pp. 176-184. [10.1016/j.conbuildmat.2018.03.233]

Availability:
This version is available at http://hdl.handle.net/11589/126357 since: 2021-03-06

Published version
DOI:10.1016/j.conbuildmat.2018.03.233

Publisher:

Terms of use:

(Article begins on next page)

17 November 2026

*Revised Manuscript
Click here to view linked References

Surface and bulk hydrophobic cement composites by tyre rubber addition

Rosa Di Mundo, Andrea Petrella, Michele Notarnicola

Department of Civil, Environmental, Land, Building Engineering and Chemistry (DICATECh)
Politecnico di Bari, via Orabona 4, 70126 Bari, Italy

Corresponding author: rosa.dimundo@poliba.it

Abstract

Penetration of water in cement composites, porous and hydrophilic materials, is cause of progressive deterioration and failure. Standard procedures for protecting building structures generally involve uniquely the modification of the surface by coating or impregnation procedures.

In this work, the addition of tyre rubber (TR) to the cement paste is demonstrated to be effective for developing mortars with a pronounced hydrophobic behavior in every part of their structure. Hydrophobic performances are better in the case of finer TR grains size and for larger TR volume addition. TR mortars show higher porosity than the conventional ones, nevertheless the effect of the low rubber surface energy prevails, and the absorption of water drops is almost completely abated. These lightweight materials result to be very competitive for non-structural applications in agreement with the environmentally sustainable policies finalized to convert a synthetic waste to an engineering resource.

Keywords: waste tyre; rubber; cement composites; mortar; hydrophobic; water absorption; water contact angle; adhesion; porosity

1. Introduction

The increasing number of vehicles on the roads of industrialised and developing nations generates millions of end-of-life (ELT) tyres (about 1.4 billion tyres are sold worldwide every year) which are a large and problematic source of waste, due to the large volume and long durability. The limited space and their potential for reuse has led many countries to impose a ban on the practice of landfilling. The estimated EU annual cost for the management of ELTs is estimated at € 600 million [1-2].

Tyre rubber is resistant to mould, heat humidity, bacterial development, ultraviolet rays, some oils, many chemicals. These characteristics, which are beneficial during on-road life, are disadvantageous in post-consumer life and boost the transformation of this material from an environmental problem to engineering resource.

One of the recovery routes involves the so called "granulate recovery" which involves tyre shredding and chipping, by which tyres are cut into small pieces of different sizes (shreds: 460-25 mm; chips: 76-13 mm; crumb rubber: 5-0.1 mm) [1]. After the removal of the steel and fabric components, the *recycled tyre rubber* (RTR) can be used for a variety of civil engineering applications such as, i.e., soft flooring for playgrounds and sports stadiums, modifier in asphalt paving mixtures or additive/aggregate to cement concrete. Among these, the addition (as crumb rubber) to asphalt mixtures is highly diffused due to the good chemical interaction, even leading to a partial dissolution [3-4].

The recovery of RTR as aggregate in cement structures has been proposed since the 90's but it is considered not convincing compared to applications in asphalt pavements [3,5]. An important reason is the not favorable interaction with the matrix. Indeed, the cement paste is mainly characterized by hydrated metal /semimetal oxides, which explains the hydrophilic nature (high surface energy) of this matrix and the good adhesion to the conventional aggregates generally based on quartz and/or limestone. Rubber, instead, made of organic polymers, is characterized by a low surface energy, and therefore by a hydrophobic character. The interaction hydrophilic-hydrophobic is very unfavorable resulting in a poor adhesion between rubber particles and the

cement matrix. Various rubber chemical treatments have been lately tested with the purpose of improving adhesion. Among these, treatments with NaOH [6-8], HNO_3 and cellulosic derivatives [9] or silane coupling agents [10] have been reported.

More importantly, lower compression resistances are always observed in rubber-cement composites with respect to the conventional ones [5,11]. This is mainly due to the fact that rubber sites are significantly softer than their surrounding media acting like ‘‘holes’’ inside the concrete. For this reason only non-structural applications have been proposed (exterior wall materials [12], pedestrian blocks, highway sound walls, residential drive ways, and garage floors [3]) and no building practice seems to be diffused.

However, an enhancement of toughness and ability to absorb impact energy has been observed (somewhere also explained and modeled), also in addition to an increased flexural strength [3,11].

Further, the lightweight character of the rubberized materials (due to the low specific weight of rubber) should be considered an advantage for the use as construction material since nowadays the structural efficiency is more important than the absolute strength level. Specifically, a decreased density for the same strength reduce the dead load, foundation size, and construction costs; it also enhances sound and thermal insulation [13].

Our objective is to focus on a specific feature of the rubber–cement composites, i.e. the low surface energy of the rubber particles which, although responsible of a low adhesion to the cement paste, should inhibit the absorption of water in artifacts.

This is a relevant applicative feature since hydrophobic cement structures have i) longer durability upon freezing-thawing cycles, as opposite to conventional porous and hydrophilic composites which, after water absorption, tend to expand on freezing thus starting cracks within the matrix; ii) self-cleaning ability; iii) resistance to paints/graffiti [14,15]. Also it has been observed how hydrophobicity can be relevant to icephobicity [16,17]. At authors knowledge this property of such composites has not been faced yet in published research.

Standard procedures for protecting cement structures are mainly based on impregnation and coating methods, involving, therefore, only the modification of exterior layers and leaving a

hydrophilic bulk [15]. Specifically, silane or siloxane are mainly used for these applications [18]. Recently, the addition of polymeric fibers to the paste mixture, combined to the use of a hydrophobic coating, has been reported to reduce water penetration and to turn to hydrophobic or over-hydrophobic nature this building material [17,19].

In this work, the effect of the TR grains addition to cement mortars has been investigated, with specific reference to wetting properties, and more specifically to contact angle and absorption of water drops. Tyre rubber was added to the mixtures formulation as partial and/or total replacement of the conventional aggregate (sand). Aiming at affordable applications of this process (addition of TR) we have tailored an addition to the cement paste without any use of additive/chemical to improve adhesion. Since the material is modified in its whole mass, and no coating is present on the surface, both the side surface and the inner (fracture) surface of the mortars/specimens are of interest. Wetting properties are correlated to the micro-scale structure (SEM) and the porosity of the specimens. Moreover, the mechanical properties of the composites are also reported.

2. Materials and methods

2.1 Mortar specimens preparation

CEM II A-LL 42.5 R, a limestone Portland cement [20] provided by Buzzi Unicem S.p.A. was used for the preparation of the cement composites. The main constituents are: 80-94% clinker, 6-20% limestone LL (<0.2% organic carbon), gypsum (0-5%), and minor additional constituents; it shows high early resistance (Rc (2 days) $_)$> 25.0 MPa, Rc (28 days) $_)$> 47.0 MPa) and Blaine specific surface area ranging 3100-4400 cm^2/g. Natural siliceous sand was provided by Societè Nouvelle du Littoral, Leucate, France with grains in the 0.08-2 mm size range [21,22].

Mortar specimens were overall prepared using this type of cement, sand, tap water (water/cement ratio kept constant at 0.5) and tyre rubber grains with particle size in the 0-2 mm range. The samples were molded in the form of prisms (dimensions 40×40×160 mm) and 28 days water cured after demolding.

112 Tyre rubber was added to the mortars formulation as partial and/or total replacement of the
113 conventional aggregate (sand). Table 1 and 2 report the aggregate and mortars composition.
114 Sand replacement was made on volume basis rather than on weight basis due to the low specific
115 weight of the lightweight materials under investigation. In order to tailor TR added mortars
116 without the addition of chemicals to improve adhesion, we previously evaluated the maximum
117 TR volume which could be incorporated into the mixture with an acceptable workability. Such a
118 volume (500 cm^3) was set as constant total volume of the aggregate. A reference, named Sand,
119 prepared by using 500 cm^3 of 0.5-2 mm sand, has been compared to the TR specimens. Total
120 sand replacement was carried out with 100 % TR grains in the 0-0.5 mm size range (TR-small),
121 100 % TR grains in the 0.5-2 mm size range (TR-large) and the last one with 50% TR grains in
122 the 0-0.5 mm and 50% 0.5-2 mm (TR-mixed). Sand-TR sample was prepared by replacing 50%
123 sand volume with TR grains in the 0-0.5 mm size range. A further conventional sand-based
124 (normalized) mortar was prepared as control [21] and indicated as Normal.
125

sample	**Type of aggregate**	
Normal	Normalized sand	
Sand	Sieved sand (0.5-2 mm) 100%	
TR-small	Rubber Tyre (0-0.5 mm) 100%	
TR-large	Rubber Tyre (0.5-2 mm) 100%	
TR-mixed	TR (0-0.5 mm) 50%	TR (0.5–2 mm) 50%
Sand-TR	Sieved sand (0.5-2 mm) 50%	TR (0-0.5 mm) 50%

126 Table 1. Aggregates composition of the mortars.
127
128
129
130
131
132

133 Table 2. Mortars compositions.

sample	cement (g)	water (cm^3)	sand volume (cm^3)	TR volume (cm^3)
Normal	450	225	810	0
Sand	450	225	500	0
TR-small	450	225	0	500
TR-large	450	225	0	500
TR-mixed	450	225	0	500
Sand-TR	450	225	250	250

134

135

136

137 *2.2 SEM/ EDX analysis and porosimetric measurements*

138 Cement-based composites were characterized by scanning electron microscope (SEM) and
139 energy dispersive X-ray (EDX) analysis. Specifically, in the case of SEM and EDX analysis,
140 used to have magnified images and the elemental composition of the samples, an electron
141 microscope FESEM-EDX Carl Zeiss Sigma 300 VP (Carl Zeiss Microscopy GmbH, Jena,
142 Germany) was used. The samples were fixed on aluminum stubs and then sputtered with gold
143 by the use of a Sputter Quorum Q150 (Quorum Technologies Ltd**,** East Sussex, UK).

144 Measurements of porosity % (parameter dependent on the total volume of the pores) were
145 carried-out by Ultrapyc 1200e Automatic Gas Pycnometer (Quantachrome Instruments,
146 Boynton Beach, FL, US). The apparatus utilises helium as inert gas which penetrates the finest
147 pores of the material thus overcoming the influence of surface chemistry. Results are the
148 average of three measurements performed onto three specimens of the same type.

149

150 *2.3 Contact Angle and water absorption measurements*

151 Contact angle measurements were performed by depositing water drops of 5 µl (a number of 5
152 drops per specimen) on the surface of the mortar specimens, both on the side surface and on the
153 fracture (inner) one. A home-made system (Premier series dyno- lyte portable microscope and
154 background cold lighting) allowed to record the evolution of the drop status in time, up to 100

s, at a frame rate of 30 frame per second. When the drop was not static (absorption took place) acquired image sequences were analysed by the Image J software (National Institute of Health, United States) in order to measure both variation of the contact angle and of the drop height after release of the drop.

2.4 Mechanical characterization

Mechanical tests were carried-out by a MATEST system, Milan, Italy. Compression resistance was carried out on samples deriving from flexural tests on 40×40×160 mm prisms after 28 days curing [21-22]. Results are the average of the measurements performed on specimens of the same type.

3. Theoretical background

In this section the terminology and the underlying theory about water contact angle and water drops penetration is briefly presented as an introductory note to readers. The term wettability refers to the ability of a surface to get wetted by a liquid, thus poor wettability refers to surfaces that tend to repel that liquid. Hydrophobic refers to surfaces that repel water, while the hydrophilic ones have favourable interactions with water. The critical parameter that is used to evaluate the wettability of a solid surface is the contact angle of the liquid on the surface. In this work the focus is only on water thus the term water contact angle (WCA) will be used throughout. A surface is considered hydrophobic if the WCA is > 90°; if WCA < 90° the surface is considered as hydrophilic. If we consider a completely smooth and chemically homogeneous surface (ideal), the chemistry of the solid surface is the only critical factor to determine its wettability, which is evaluated by the Young equation:

$$\cos \vartheta = \frac{\gamma_{SG} - \gamma_{SL}}{\gamma_{LG}} \qquad (1)$$

]where ϑ is the contact angle (CA) of the liquid (water) droplet on the solid surface and γ_{SG} is the solid-vapor interfacial energy, γ_{SL} is the solid-liquid interfacial energy and γ_{LG} is the liquid-

vapor interfacial energy[23]. For a given smooth surface, proper design of its chemistry is able to tailor the desired surface energy, i.e. the solid-vapor interfacial energy γ_{SG}, hence the desired ϑ [24]. If the solid surface is not smooth, or equivalently a certain roughness is present, the apparent contact angle differs from ϑ. Basically speaking for an inherent hydrophobic surface (low surface energy), an increase of surface roughness leads to an increase of hydrophobicity translated to higher apparent WCA. On the other hand, for an inherent hydrophilic surface an increase of surface roughness leads to an increase of hydrophilicity translated to lower apparent WCA [25-26]. This implies that the WCAs measured on the surfaces in this work, never ideally smooth, are apparent contact angles. However, it should be noted that the effect of roughness, for the composite materials under focus, can be considered at a first analysis less important than chemical non-homogeneity and porosity in driving wetting behaviour.

Regarding porosity, in the simple case of only one pore under the drop and with borders with a homogeneous chemistry (i.e. surface energy), the drop stands/is in equilibrium if the forces directed downwards (force due to Laplace pressure at the curved drop surface and gravitational force) are balanced by the meniscus tension on the pore perimeter (the one producing capillary pressure). The latter for fully hydrophobic materials is directed upwards, while for fully hydrophilic materials is directed downwards. In general [27-28], penetration occurs when net force F_{net}, given by the three terms (from left to right) expressing the force due to Laplace pressure, the gravitational force, and the force due to the meniscus on the pore perimeter is greater than zero that is:

$$F_{net}=\frac{\pi\gamma d^2}{2R_d}+\rho g R_d(1-cos\vartheta)\frac{\pi d^2}{4}+\pi d\gamma cos\vartheta > 0 \qquad (2)$$

Here ϑ is the contact angle of the drop on the surface, d is the pore diameter, R_d the drop radius, γ is the surface tension of water , ρ is density of water, g is the gravitational acceleration, and $R_d(1-cos\vartheta)$ is the height of the drop. Thus in this simple case of only one and chemically homogeneous pore under the drop the parameters affecting motion of the drop are d, R_d, ϑ.

4. Results and discussion

A picture of the specimens, on the left the Sand reference and on the right a TR mortar (TR-small) is presented on the left of **figure 1**.

Characterization was performed both on the side and on the inner surface of the mortars. The inner surface results from the fracture of the specimens occurring upon compression tests. A magnified micrograph of a TR added sample can be appreciated on the right of figure 1. Side and fracture surface are very different for both the reference sand samples and the TR added ones. The side surface is almost homogeneously made of cement paste which, when fluid, can better fill the space close to the mold surface. The fracture surface, instead, beside being rougher, as a consequence of fracture, is characterized by a visible distribution of aggregates (sand and /or TR grains) embedded in the cement paste.

Wetting results of the reference Sand sample are reported in figure 2 (side surface) and 3 (fracture surface). **Figure 2** diagrams report water contact angle (WCA) and drop height as a function of time measured on the side surface in 5 different positions. A very different behavior is observed on the various points: slow absorption in points 1 and 2, with the drop penetrating below the surface in more than one minute; fast absorption in point 5, where a full penetration occurs in few seconds; hydrophobic behavior in point 3 where the drop is completely stable with a relatively high angle (120°, typical of hydrophobic solids such as Teflon [29]). When penetration occurs, WCA generally follows the trend of the drop height: as the drop penetrates (hence, as the height decreases) the contact angle also goes down, i.e. the drop spreads over the surface. It means that the drop penetration in the composite proceeds in all the directions, both orthogonal and parallel to the surface.

Results on the fracture surface of the reference sample are reported in **figure 3**. In this case a very fast absorption is observed over all the tested points, with full penetration occurring even in less than half second. Also in this case measurement of the WCA (not easy in this case due to the macro-scale roughness of the surface and the very spread shape of the drop) follows the

trend of the drop height, thus a very fast spreading occurs together with the absorption. This surface can be considered superhydrophilic [26] and fast absorbent. Almost identical results (both on the surface and on the bulk) are observed on the standard N reference mortar (Normal).

It is reasonable to consider the behavior of the fracture surface as the one truly representative of conventional mortars/concrete since representing a section of the artifacts with all the components (cement paste and sand) and with an intrinsic porosity, i.e. not altered by the local effect. It should be noted that as soon as the side surface undergoes wear, scratching or any other damage, the inner material is disclosed and exposed to environment.

Wetting characterization results of TR mortars, specifically with small fraction TR size (TR-small), are reported in **figure 4**. As described above, TR grains are added to the cement mixture in total replacement of the sand volume. In this case both for the side surface (on the top) and the fracture surface (on the bottom) only the drop height is diagramed, as the WCA trend is very similar. It is absolutely interesting to appreciate that both on the side and on the fracture surface the drop is stable on the surface (except a minimum height decrease in one point) for all the observation time. The WCAs are nearly stable as reported in the diagram box; WCAi are the initial values for the points where a slight variation has been observed. WCA values are always above 100 °, and in some cases even reaching 125°, on the side surface and above 90° on the fracture one. This wetting behavior can be classified as from hydrophobic (WCA > 90°) to overhydrophobic (WCA> 120°) and is that typical of the most hydrophobic among organic polymers, such as PTFE (polytetrafluoroethylene) or PDMS (polydimethylsiloxane) [23,29]. Thus the presence of rubber prevails and makes ineffective the presence of the hydrophilic cement regions in these mortars.

A comparison among this sample and the other TR- mortars (TR-large and TR-mixed) is reported in **figure 5**, with the optical micrographs of the respective fracture surfaces at the top and an histogram (at the bottom) reporting the water drop entry % (percent difference between initial and final (at 100s) drop height). For every sample and every surface (with S as side, and F as fracture) the water drop entry is averaged over the measurements of the five drops. Results related to the Sand reference sample (presented in detail in figure 2) are here reported on the

261 average for comparison. As it can be appreciated all the TR-mortars present a pronounced
262 abatement (more than 80%) of the water absorption. Among these, the specimen fabricated with
263 smaller fraction rubber aggregates (TR-small) shows the best performance (more than 95%),
264 reasonably as a consequence of a denser distribution of hydrophobic sites on the surface.
265 Regarding this point it should be noted that under our conditions the contact area between water
266 and the sample surface is at least about 2 mm (as in the case of highly hydrophobic interaction,
267 as in the pictures of figure 4); the samples with larger grain size fraction (TR-large and TR-
268 mixed), since the total volume is constant, are also characterized by a lower number of particles.
269 Therefore, larger hydrophilic (cement paste) spaces are available where a slight access to water
270 is possible (optical micrographs in **figure 5** clarifies this aspect).
271 The possibility of using rubber and sand in the same mortar has been also tested with the aim to
272 combine the advantages of the standard sand aggregate and the features of rubber.
273 The behavior of mortars prepared by replacing 50% sand volume (Sand-TR-mortars) is reported
274 in **figure 6.** The optical micrograph on the top shows on the fracture surface distinguishable
275 sand grains together with the TR ones. Water absorption (water drop entry % in the diagram at
276 the bottom) is also significantly abated with respect to the reference samples, however it is
277 appreciably higher than the TR-mortars. Reasonably this less effective hydrophobization is due
278 to the halved volume of rubber, more than to the introduction of sand, which, is a hydrophilic
279 but non porous material.
280 In **figure 7** the inflection and compression resistance of these samples are reported as a function
281 of the specific weight. In particular, we find that total replacement of sand with TR grains
282 results in halving the specific weight with respect to the sand mortar. Moreover, the inflection
283 resistances and the compression resistances are sensitively lower than the reference sample.
284 Replacement of 50% sand volume with TR grains leads to an increase of the specific weight and
285 of the mechanical resistances with respect to the 100% sand replacement. Porosity % (by
286 Helium picnometer, sensitive to the total volume of the pores) of all these samples is reported in
287 **figure 8** diagram as a function of TR volume ratio. Three markers at 100% TR are related to the
288 three different TR grain size fractions. Indipendently of the rubber particle size fraction,

289 porosity turns out doubled with respect to the sand reference. Porosity of the TR-sand specimen
290 is also considerably higher than the reference. Overall, these results confirm the lightening and
291 pore-generating effect of the rubber aggregates, diffusively reported in literature, as described in
292 the introduction section. This can be considered an advantage in terms of building efficiency
293 [13]and suggests non structural and thermal insulating applications for these composites.
294 The porosity results can be explained by the SEM images reported in **figure 9.** Specifically,
295 rubber grains have an intrinsic micro-scale texture and porosity ("as received" rubber particle is
296 reported on the top). Further, as a consequence of the unfavorable adhesion between rubber and
297 cement paste, thoroughly discussed in introduction section, we also have verified the presence
298 of large voids around the rubber grains. The other images are those acquired on the sand
299 reference (middle) and on a TR-mortar (bottom). The length of the voids can reach the
300 dimensions of the TR grains (i.e. order of mm) and the width can be even 20-30 micron. This
301 effect has been also reported by other authors [30, 31]. EDX analysis have been performed to
302 have a detailed composition of the different regions of the composites. Basically, sand
303 composition is: C (4%), O (52%), Si (35%), Ca (2%); rubber composition is: C (25%), O (70%),
304 S (1.5%); cement paste composition is: C (5%), O (40%), Si (7%), Ca (40%), Fe (1%), Al (1%).
305 The porosity induced by rubber sites in this matrix could also increase water permeability [32].
306 However, these sites decrease the mean surface energy and our results show that this effect
307 prevails on the increased porosity in terms of mortar water penetration.
308 Penetration of water drops into hydrophobic pores is recently under study with the aim to
309 predict the behavior of such drops. Choi and Liang [33] have shown, with reference to eq. 2,
310 that onto fully hydrophobic surfaces with single or multiple pores with a set diameter the
311 smaller the drops (in the range 0.5-15 μl) the less unfavorable the penetration is, since the
312 Laplace pressure can get larger than the meniscus force. For instance, 5 μl drops can penetrate
313 into a fully hydrophobic material (polydimethylsiloxane, angle of about 110°) if the pores
314 diameter is greater than 500 μm. In our case the surface is a composite matrix of hydrophilic
315 porous domains (cement paste) mixed to hydrophobic ones (rubber). Sand grains, when present,
316 represent hydrophilic but non porous domains. Thus these composites have multiple contact

angles: a hydrophobic contact angle (and meniscus angles) which is around 90 °, as it has been measured on a flat sheet of tyre rubber, and a plurality of angle values in the hydrophilic field (lower than 70°, also down to 5-10 °) relative to the cement paste and, eventually, sand grains. Further, the pore diameter in the cement matrix spans in a very large range, from the nano- and micro-scale scale [34, 35] to the macro-scale pore as those shown in the SEM) characterization. Modeling this problem is therefore not straightforward and could be of high interest for next studies. What we experimentally found is that with less than 50% surface area made of hydrophobic matter (as it can be observed in optical images in figure 5) it is possible to get an overall behavior of the composite material which is fully hydrophobic. A simplified scheme sketching the status of a water drop on the surface of these composites is presented in **figure 10**.

Conclusions

In this work, it was evaluated the possibility of exploiting the low surface energy of tyre rubber in order to induce protection in cement composites against penetration of water drops. Results show that tyre rubber addition in cement mortars strongly abates penetration of small water drops which goes from 100% in conventional specimens to 3-5 % in the rubberized ones. Surface and bulk of these materials have very different structure and composition, nevertheless they show a similar waterproof behavior. This means that the property exists in the whole material and cannot be modified by eventual wear or damage events of the surface.

Maximum hydrophobic performances are found when the average size of the tyre rubber grains size is finer and their total volume in the mixture is larger, i.e., after total replacement of the conventional sand aggregate.

Interestingly, the hydrophobic character of the rubber, although increasing the porosity of the mortars due to the limited adhesion to the cement paste, and in spite of the presence of hydrophilic porous domains (cement) at the water-solid interface (more than 50% surface area), prevails in nullifying the net force for penetration and stabilizing the deposited drops on the surface.

Application in construction of tyre-rubber cement composites, already suggested for non-structural and thermal insulating uses due to the lightweight and porous character, is now strengthened by the hydrophobic behaviour here documented.

In particular, in light of such a property, they could find suitable applications in buildings as i) plasters for outside walls and in general for vertical elements exposed to water flowing and capillary rise, or ii) screeds for flat roofs and/or balconies. Other possible construction applications, beside the already suggested sidewalks and playground pavements, are coatings for tanks and gutters. Further work will be surely necessary in order to developing every mentioned construction application, both in terms of specifics standard characterizations and in terms of eventual admixture optimization. However, these results first demonstrate a material performance arising from the combination of rubber with a cement matrix. Finally, considering the re-used origin of this material, it is easy understandable that tyre rubber-cement composites are also cost-effective construction materials and in perfect agreement with the current policies of environmental sustainability.

Acknowledgments

Rosa Di Mundo gratefully acknowledges the Future in Research Program of the Apulia Region (Fondo di Sviluppo e Coesione 2007-2013 – APQ Ricerca Regione Puglia "Programma regionale a sostegno della specializzazione intelligente e della sostenibilità sociale ed ambientale").

The authors acknowledge Adriano Boghetich and Ernesto Robertiello for the technical support in specimens preparation, Marianna Gaudio and Priscilla Amodio for the asistence in data analysis, Stefania Liuzzi and Pietro Stefanizzi for the porosity measurements.

References

[1] D. Lo Presti, Recycled Tyre Rubber modified bitumens for road asphalt mixtures: a literature overview, Constr. Build. Mater. 49 (2010) 863-881.

[2] End of Life Tyres. http://www.etrma.org/uploads/Modules/Documentsmanager/brochure-elt-2011-final.pdf , 2011 (accessed 08 October 2017).

[3] X. Shu, B. Huang, Recycling of waste tyre rubber in asphalt and portland cement concrete: an overview, Constr. Build. Mater. 67 (2014) 217–224.

[4] M. Heitzman, design and construction of asphalt paving materials with crumb rubber modifier, Transport. Res. Record: J. transport Res. Board. 1339 (1992) 1-8.

[5] B.Huang, G. Li, S.S. Pang, J. Eggers, Investigation into waste tyre rubber-filled concrete, J. Mater. Civ. Eng. 16 (2004) 187-194.

[6] N. Segre, I. Joekes, Use of tyre rubber particles as addition to cement paste, Cem. Concr Res. 30 (2000) 1421–1425.

[7] G. Li, M. A. Stubblefield, G. Garrick, J. Eggers, C. Abadie, B. Huang, Development of waste tyre modified concrete, Cem. Concr. Res. 34 (2004) 2283–2289.

[8] G. Li, G. Garrick, J. Eggers, C. Abadie, M. A. Stubblefield, S.S. Pang, Waste tyre fiber modified concrete, Compos. Part B: Eng. 35 (2004) 305-312

[9] B. I. Lee, L. Burnett, T. Miller, B. Postage, J. Cuneo, Tyre rubber/cement matrix composite, J. Mater. Sci. Lett. 12 (1993) 967-968

[10] G. Li, Z. Wang, C. K. Y. Leung, S. Teng, J. Pan, W. Huang, E. Chen, Properties of rubberised concrete modified by using silane coupling agent and carboxylated SBR, J. Clean. Prod. 112 (2016) 797-807.

[11] N.N. Eldin, A.B. Senouci, Rubber-tyre practices as concrete aggregate, J. Mater. Civ. Eng. 5 (1993) 478–96.

[12] H. Zhu, T. Noresit, X. Zhang, Adding crumb rubber into exterior wall materials, Waste Manage Res. 20 (2002) 407-13.

[13] V. Corinaldesi, A. Mazzoli, G. Moriconi, Mechanical behaviour and thermal conductivity of mortars containing waste rubber particles, Mater. Des**.** 32 (2011) 1646-1650.

[14] E. Neto, S. Magina, A. Camoes, L. P. Cachim, A. Begonha, D. V. Evtuguin, Characterization of concrete surface in relation to graffiti protection coatings, Constr. Build. Material. 102 (2016) 435-444

[15] S. Weisheit, S.H. Unterberger, T. Bader, R. Lackner, Assessment of test methods for characterizing the hydrophobic nature of surface-treated High Performance Concrete, Constr. Build. Mater. 110 (2016) 145-153

[16] R. Ramachandran, M. Kozhukhova, K. Sobolev, M. Nosonovsky, Anti-Icing Superhydrophobic Surfaces: Controlling Entropic Molecular Interactions to Design Novel Icephobic Concrete, Entropy 18 (2016) 132.

[17] R. Ramachandran, K. Sobolev, M. Nosonovsky, Dynamics of Droplet Impact on Hydrophobic/Icephobic Concrete with the Potential for Superhydrophobicity, Langmuir. 31 (2015) 1437-1444

[18] EN 1504-2, Products and systems for the protection and repair of concrete structures. Definitions, requirements, quality control and evaluation of conformity in: Part 2: Surface Materials and structures protection systems for concretes, BSI, Brussels, 2004.

[19] I. Flores- Vivian, V. Hejazi, M. I. Khozhukova, M. Nosonovsky, K. Sobolev, Self-Assembling Particle-Siloxane Coatings for Superhydrophobic Concrete, ACS Appl. Mater. Interfaces. 5 (2013) 13284-13294

[20] Cement Composition, Specifications and Conformity Criteria for Common Cements. EN 197-1, http://store.uni.com/magento-1.4.0.1/index.php/en-197-1-2011.html,2011 (accessed 14 September 2011).

[21] Methods of Testing Cement-Part 1: Determination of Strength. EN 196-1, http://store.uni.com/magento-1.4.0.1/index.php/en-196-1-2016.html, 2016 (accessed 27 April 2016).

[22] Cement, test methods, determination of strength. ISO 679, http://store.uni.com/magento-1.4.0.1/index.php/iso-679-2009.html,2009 (accessed 24 April 2009).

[23] F.Palumbo, R. Di Mundo , Wettability: Significance and measurement, in: L. Sabbatini (ed.) Polymer Surface Characterization, De Gruyter, Berlin, 2014, pp. 207-241.

[24] R. Di Mundo, F. Palumbo, R. d'Agostino, Influence of chemistry on wetting dynamics of nanotextured hydrophobic surfaces, Langmuir 26.7 (2009): 196-5201.

[25] R. Di Mundo, F. Bottiglione, G. Carbone, Cassie state robustness of plasma generated randomly nano-rough surfaces, Appl. Surf. Sci.,16 (2014) 24-332.

[26] R. Di Mundo, R. D'Agostino, F. Palumbo, Long-Lasting Antifog Plasma Modification of Transparent Plastics, ACS Appl. Mater. Interfaces. 6 (2014) 17059-17066.

[27] A. Marmur, Penetration and displacement in capillary systems of limited size, Adv. Colloid Interface Sci. 39 (1992) 13–33.

[28] P. Yue, Y. Renardy, Spontaneous penetration of a non-wetting drop into an exposed pore, Phys. Fluids 25 (5) (2013) 052104.

[29] N. Menga, R. Di Mundo, G. Carbone, Soft-Blasting of fluorinated Polymers: the easy way to superhydrophobicity, Mater Design. 121 (2017) 414-420.

[30] A. Turatsinze, S. Bonnet, J. L. Granju, Mechanical characterisation of cement-based mortar incorporating rubber aggregates from recycled worn tyres, Build. Environ. 40 (2005) 221-226.

[31] N. Segre, I. Joekes, Use of tyre rubber particles and addition, Cem. Concr. Res. 30 (2000) 1421–1425.

[32] D. M. Roy, P. W. Brown, D. Shi, B.E. Scheetz, W. May, Concrete microstructure porosity and permeability, ARRB Group Lim, 1993.

[33] H. Choi, H. Liang, Wettability and spontaneous penetration of a water drop into hydrophobic pores, J. Colloid Interface Sci. 477 (2016) 176–180.

[34] X. Chen, S. Wu, Influence of water-to-cement ratio and curing period on pore structure of cement mortar, Constr. Build. Mater. 38 (2013) 804–812.

[35] R. Kumar, B. Bhattacharjee, Porosity, pore size distribution and in situ strength of concrete, Cem. Concr. Res. 33 (2003) 155-164.

Figure 1

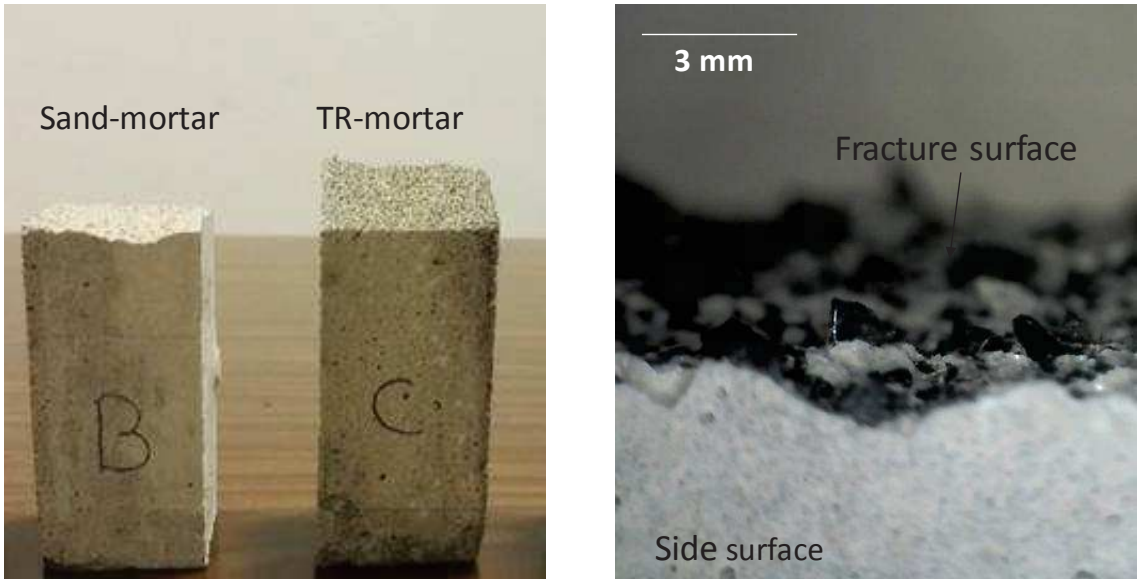


Figure 1. Picture of a sand based mortar (Sand reference) and TR added mortar (left); micrograph of the side and fracture surface of a TR added mortar.

Figure 2

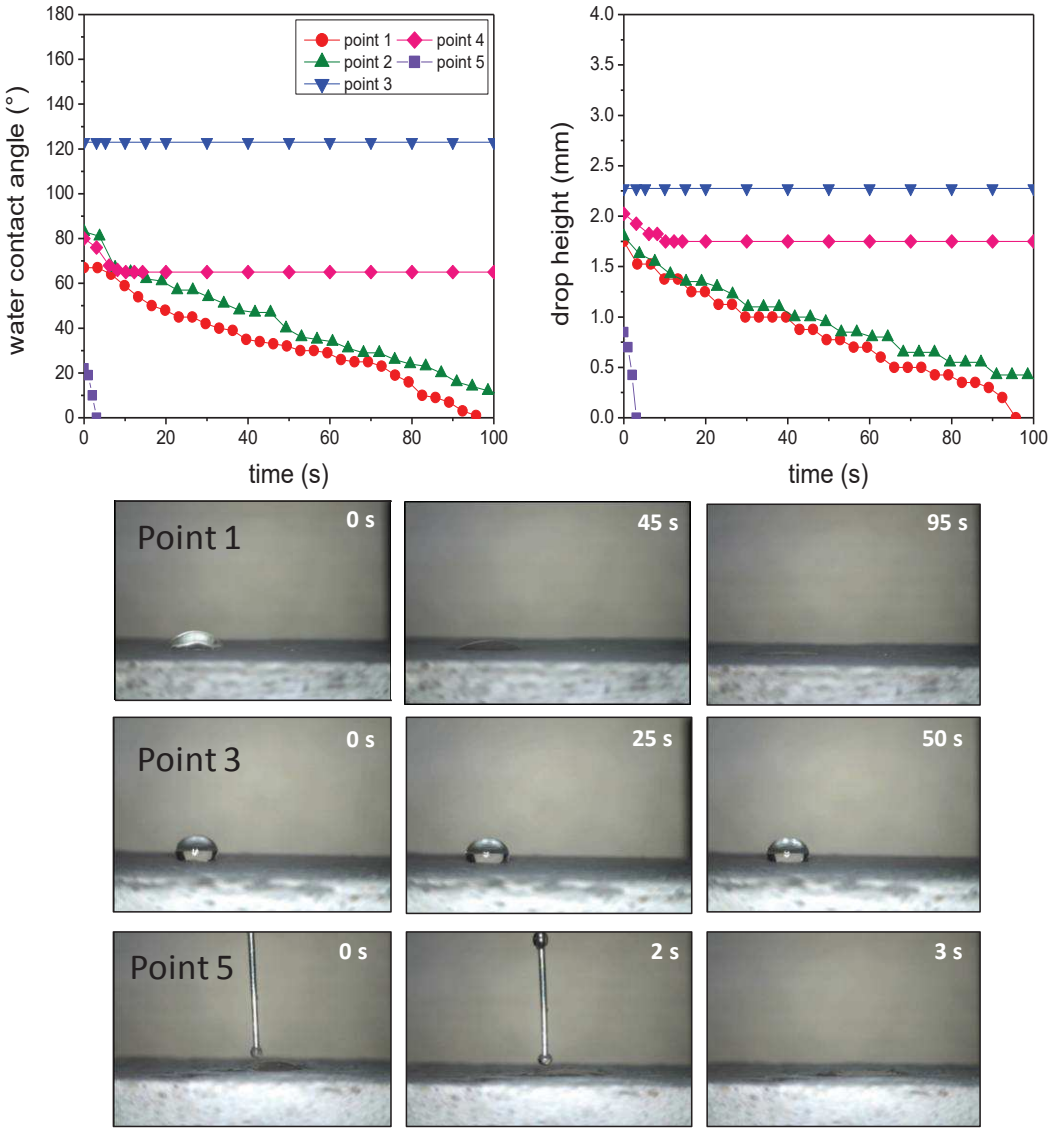


Figure 2: WCA and drop height as a function of time in the case of the side surface of the Sand reference mortar.

Figure 3

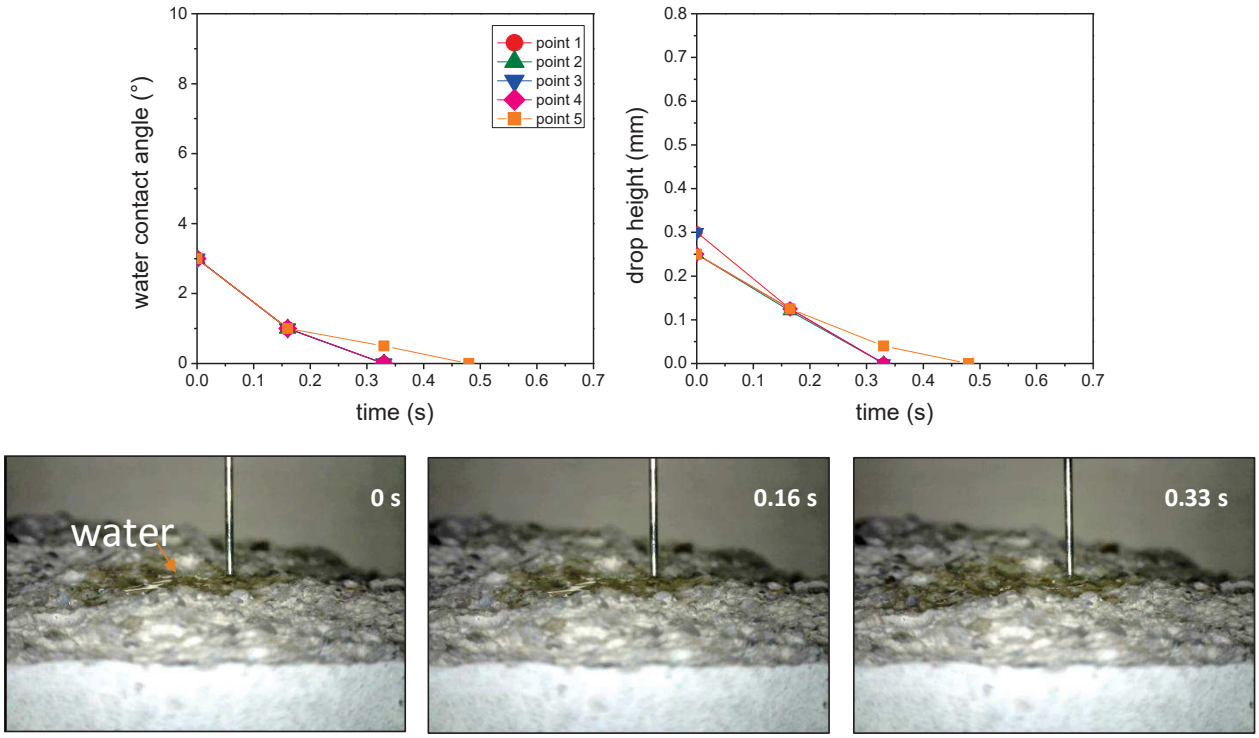


Figure 3: WCA and drop height as a function of time in the case of the fracture surface of the Sand reference.

Figure 4

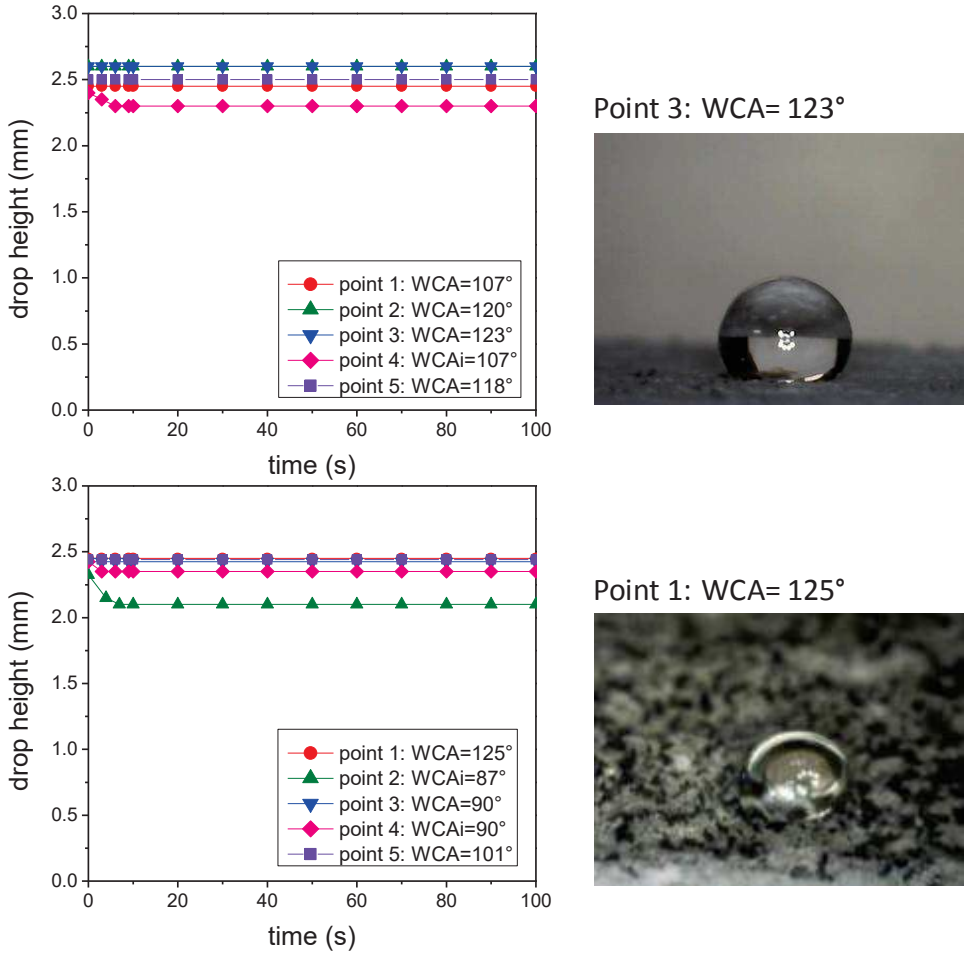


Figure 4: Drop height as a function of time in the case of the side surface (top) and of the fracture surface (bottom) of the TR-small sample. WCA values are reported in the diagrams legend. On the right, for each surface, a picture of the drop is reported related to one of the tested points.

Figure 5

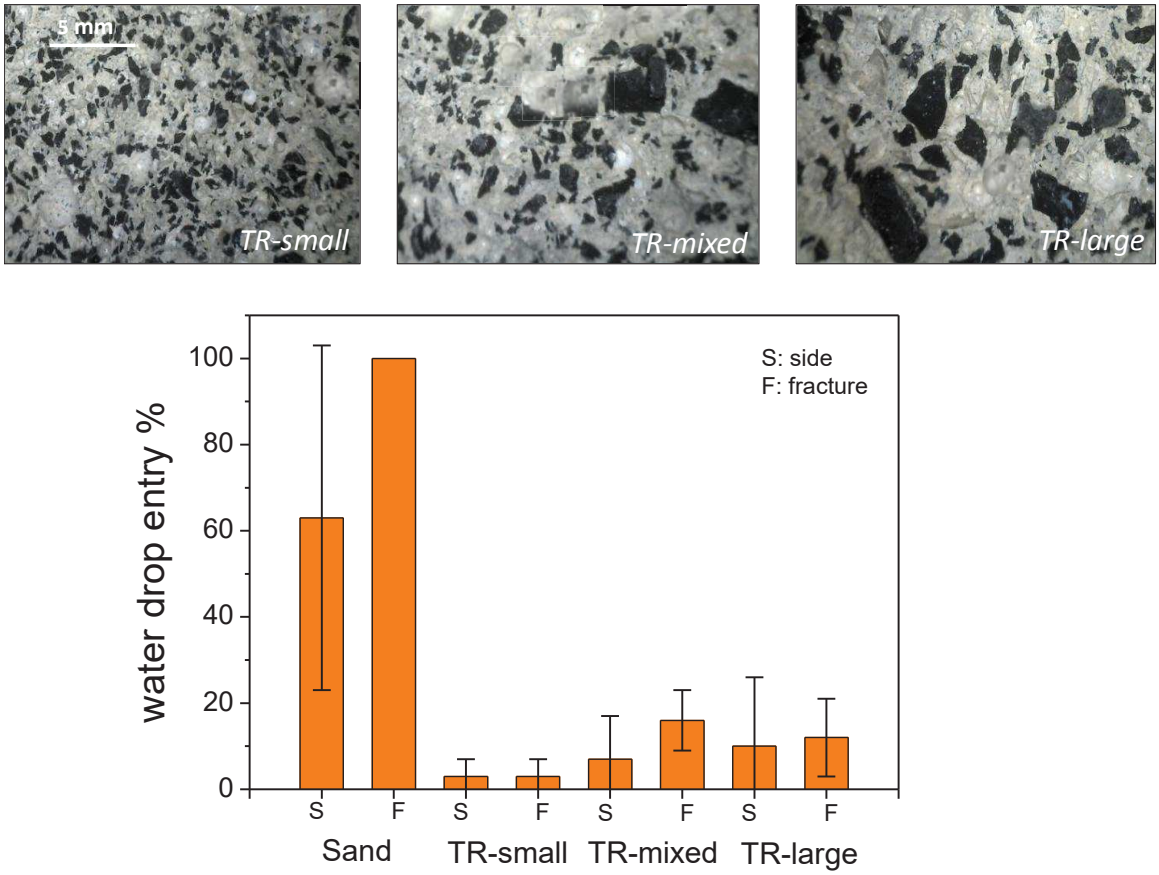


Figure 5: Water drop entry (%) in the case of the side and the fracture surfaces of the Sand reference, TR-small, TR-mixed, and TR-large samples. On the top: optical micrographs of the TR-samples.

Figure 6

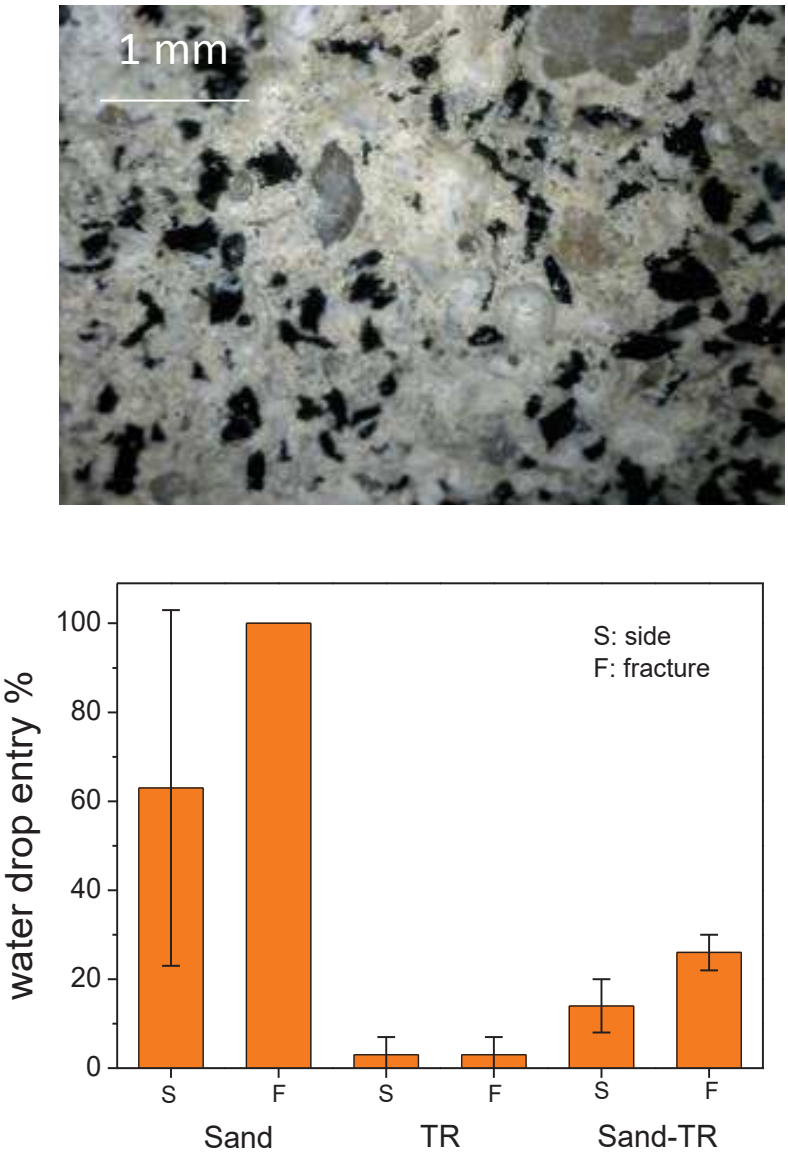


Figure 6: (top) Optical micrograph of the Sand-TR-sample. (bottom) Water drop entry (%) in the case of the side and fracture surfaces of the Sand reference, TR-small sample and Sand-TR sample.

Figure 7

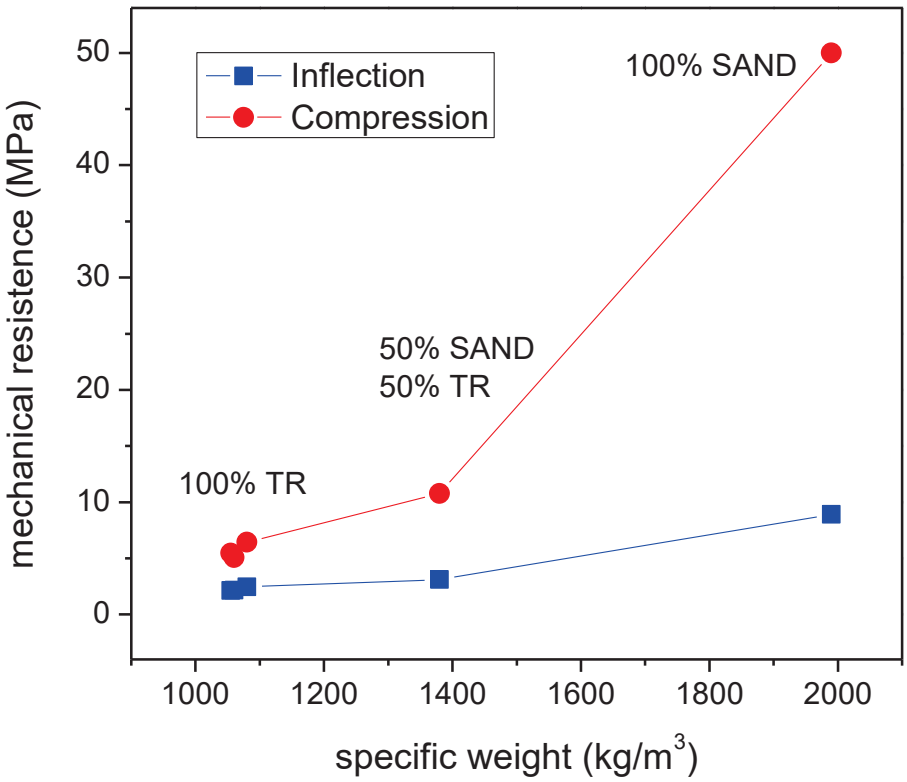


Figure 7: Mechanical resistances of the samples as a function of the specific weight.

Figure 8

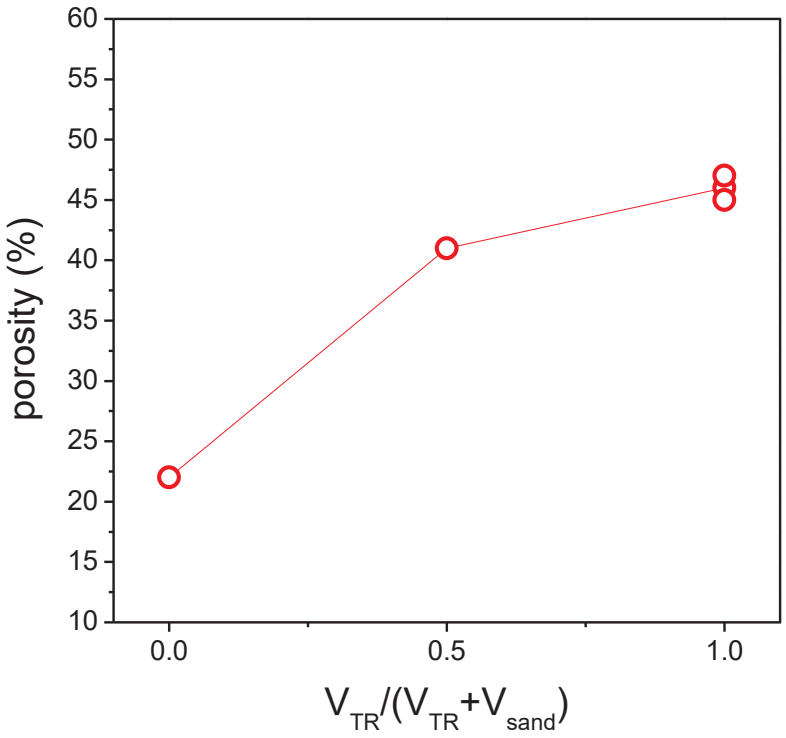


Figure 8: Porosity (%) of the samples as a function of TR volume ratio.

Figure 9

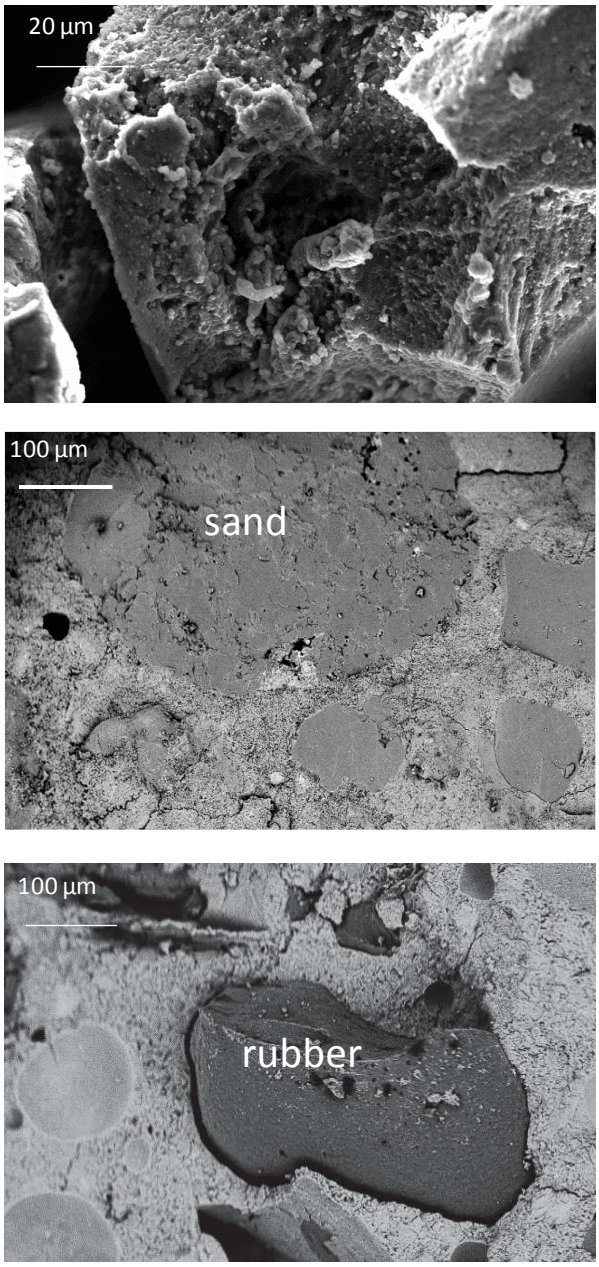


Figure 9: SEM images of a“as received” tyre rubber grain (top), Sand reference (middle), TR-small specimen (bottom)

Figure 10

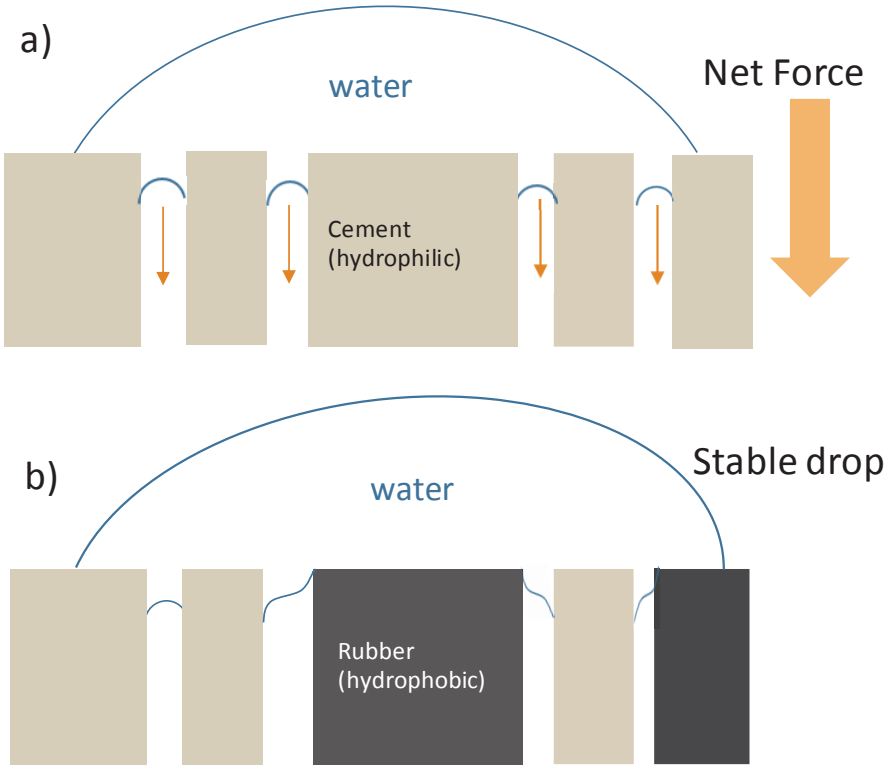


Figure 10: Scheme sketching the drop on the surface of a) conventional (sand based) mortar with a surface uniquely made of high surface energy (hydrophilic) domains at various degree and b) a mortar containing tyre rubber grains, thus having a surface composed of very high surface energy (hydrophilic) and very low surface energy (hydrophobic) domains.